PERGAMON

Computers & Fluids 28 (1999) 63–86

computers & fluids

On the behaviour of upwind schemes in the low Mach number limit

Hervé Guillard, Cécile Viozat *

INRIA, BP 93, 06902 Sophia Antipolis Cedex, France

Received 9 April 1997; received in revised form 29 November 1997

Abstract

This paper presents an asymptotic analysis in power of the Mach number of the flux difference splitting approximation of the compressible Euler equations in the low Mach number limit. We prove that the solutions of the discrete system contain pressure fluctuations of order of the Mach number while the continuous pressure scales with the square of the Mach number. This explains in a rigorous manner why this approximation of the compressible equations fails to compute very subsonic flow. We then show that a preconditioning of the numerical dissipation tensor allows to recover a correct scaling of the pressure. These theoretical results are totally confirmed by numerical experiments. © 1998 Elsevier Science Ltd. All rights reserved.

Keywords: Low Mach number; Flux difference splitting upwind schemes; Roe scheme; Preconditioning

1. Introduction

The computation of low Mach number flows is continuing to be a challenge for compressible flow solvers and a general algorithm valid for all flow speeds is still to be found. While many different flow regimes can be encountered for small Mach number [1], this paper considers exclusively the simple case where the solutions of the equations for compressible flows converge to solutions satisfying the equations for incompressible flows. From a theoretical point of view, the situation is now well understood in the inviscid case: if the initial pressure field scales with the square of the Mach number: $p(\boldsymbol{x}, 0) = P_0 + M_*^2 p_2(\boldsymbol{x})$, and if the velocity field at time $t = 0$ is close to a divergence free field: $\boldsymbol{u}(\boldsymbol{x}, 0) = \boldsymbol{u}_0(\boldsymbol{x}) + M_* \boldsymbol{u}_1(\boldsymbol{x})$ with $div(\boldsymbol{u}_0) = 0$, then it is known that the solutions of the equations for compressible flows remain uniformly bounded as the

* To whom correspondence should be addressed.

0045-7930/99/$ - see front matter © 1998 Elsevier Science Ltd. All rights reserved.
PII: S0045-7930(98)00017-6

Mach number tends to zero, and that the limit solutions satisfy the equations for incompressible flows. A rigorous proof of this result can be found in Ref. [2], while a general treatment of hyperbolic problems exhibiting different time scales can also be found in works by Kreiss, Gustafsson and their co-workers (see Refs [3, 4]). These last works point out that with proper initialization (see for instance Ref. [5], where it is shown how to construct initial data such that the solution and their derivatives remain bounded independently of the 'small parameter') the solutions of the complete equations converge to solutions satisfying a set of 'reduced' equations that for fluid dynamics problems are the incompressible Euler equations.

However, if on the continuous case, the situation is clear, in the discrete case, the problem of finding on a fixed grid an approximation of the equations for compressible flows whose accuracy will not deteriorate as the Mach number decreases, is still a problem of great practical and theoretical interest.

Actually, it is well known that in addition to convergence and round-off error difficulties, the approximations of the compressible fluid flow equations suffer from accuracy problems in the low Mach number limit. There are experimental evidences showing that on a fixed mesh, the discretized solution of the compressible fluid flow equations are not an accurate approximation of the incompressible equations (e.g. see Refs [6, 7]).

A common explanation of this failure of the compressible solvers is to put forward the role of the numerical dissipation. In this paper, we are interested in upwind schemes, where the numerical dissipation associated with the two grid nodes $\boldsymbol{i}$ and $\boldsymbol{l}$ is of the form:

$$\delta \mid \mathbf{A} \mid \Delta_{il} q = \delta \sum_i \mid \lambda_i \mid \alpha_i(\Delta_{il}) \mathbf{R}_i, \tag{1}$$

with δ the mesh size, λ_i and $\mathbf{R}_i$ respectively the eigenvalues and eigenvectors of the Jacobian matrix $\mathbf{A}$, $\alpha_i(\Delta_{il})$ the coordinate of the jump $\Delta_{il}q$ between the values of the function q at the grid nodes $\boldsymbol{i}$ and $\boldsymbol{l}$ in the basis formed by the eigenvectors. In the above expression, the sum runs over all waves. If we introduce a reference Mach number M_* we see that this implies that some of the wave speeds λ_i become proportional to $1/M_*$. Thus, in the low Mach number limit these terms can grow without bound, resulting in an excessive numerical dissipation that pollutes the discrete solution.

We believe that this explanation is only partially true and needs to be refined. Firstly, we remark that, if the dissipative terms are of order $1/M_*$, the centred terms in the approximation scale with $1/M_*^2$ (see Section 2). Thus, although the amplitude of the dissipative terms may go to infinity, they become negligible with respect to the centred ones as M_* goes to zero. Therefore, the accuracy problem may actually result from a lack of numerical dissipation, instead of resulting from an excess of numerical viscosity. Note that this fact has been observed before in related work carried out by Turkel, Fitermann and Van Leer [8], where for scalar numerical viscosity it was observed that a density based viscosity gives a numerical dissipation term that is too small. Secondly, in upwind schemes, the numerical dissipation is a 4×4 tensor (in 2D) and although some of the λ_i goes to infinity, it may well be that the discrete equations force the associated jumps α_i (Δ_{il}) to go to zero.

Our aim in this work is thus to explain in a detailed manner the mechanism by which compressible upwind schemes fail to compute very subsonic flows. The tool we will use for this study is only a standard asymptotic analysis in power of the Mach number. However, this

analysis will be performed on *the discrete equations* instead of the continuous ones. More specifically, we will look for the asymptotic form that takes the discrete system in the low Mach number limit. The analysis we performed is a fully non-linear one that does not require any linearization of the governing equations. Moreover, it applies to the steady-state equations as well as the time-dependent ones. Its main result can be stated as follows: in the low Mach number limit, the solution of the discrete equations contains pressure fluctuations of the order of the Mach number. This is in clear contrast with the continuous case, where pressure fluctuations scale with the square of the Mach number.

For the steady-state equations, a common strategy to overcome the convergence problems encountered by compressible solvers is the use of preconditioning [8–12]. Following a suggestion in Ref. [8], we tried in Ref. [13] to use preconditioning as a cure to the accuracy problem. The results were extremely convincing and it appears that preconditioning is a powerful remedy to cure the accuracy problem. More specifically, the dissipative term in Eq. (1) $\delta|\mathbf{A}|\Delta q$ is changed into:

$$\delta\mathbf{P}^{-1} \mid \mathbf{PA} \mid \Delta q \tag{2}$$

where $\mathbf{P}$ is the preconditioning matrix. However, the temporal and centred terms of the approximation remain unchanged (i.e. with no preconditioning). Therefore, the scheme is always consistent with the time-dependent equations and only the numerical dissipation is altered. Although more complex than in the case with no preconditioning, an asymptotic analysis of the resulting discrete equations is tractable. It provides a detailed explanation of the mechanism by which preconditioning increases the accuracy of the schemes. In particular, it shows that preconditioning increases the numerical dissipation terms associated to the continuity and energy equations by a factor of $1/M_*$. Since the original non-preconditioned equations contain terms of order $1/M_*$, the resulting preconditioned system contains only terms of order $1/M_*^2$ and 1, as in the continuous case. Solving these equations gives pressure that possesses the same M_*^2 scaling as for the continuous system.

The analysis presented in this work uses Roe's approximate Riemann solver. This scheme possesses some nice algebraic features that simplify, to some extent, the discrete equations. However, the analysis is general and applies to all the schemes that can be cast under the form in Eq. (1), with a matrix $\mathbf{A}$ that is the Jacobian of the continuous fluxes evaluated at some average between $\boldsymbol{i}$ and $\boldsymbol{I}$. The outline of this paper is as follows: in the next section, we recall how to derive the convergence of the compressible Euler equations toward the incompressible ones. Next, we apply the same asymptotic expansions as in the continuous case to the discrete Roe scheme, and finally, in the last section, we examine the case of a preconditioned dissipation.

2. The continuous case

In this section, we recall how to derive in a formal way, the singular limit of the compressible Euler equations when the Mach number goes to zero. This situation is studied in detail in Ref. [2] or with different approaches in Refs [3, 4].

In particular, a detailed and rigorous proof including energy estimates can be found in Ref. [2]. This proof uses the isentropic compressible equations, since in the low Mach number limit, one can safely assume that no shock waves are present and the energy equation and state law can be replaced by the relation $p/\rho^{\gamma} = \text{constant}$. Here, although we essentially follow the formal derivation given in Ref. [2], we prefer to use the complete non-isentropic compressible system to point out the differences with the system obtained after discretization of these conservative equations.

The equations of motion of inviscid compressible fluids are:

$$\frac{\partial}{\partial t}\rho + \mathrm{div}(\rho\vec{\boldsymbol{u}}) = 0, \tag{3}$$

$$\frac{\partial}{\partial t}\rho\vec{\boldsymbol{u}} + \mathrm{div}(\rho\vec{\boldsymbol{u}} \otimes \vec{\boldsymbol{u}}) + \nabla p = 0, \tag{4}$$

$$\frac{\partial}{\partial t}\rho e + \mathrm{div}(\rho e\vec{\boldsymbol{u}} + p\vec{\boldsymbol{u}}) = 0, \tag{5}$$

where ρ is the fluid density, $\vec{\boldsymbol{u}}$ the velocity and e the total energy, defined as the sum of the internal energy plus the kinetic energy.

$$e = C_v T + \frac{1}{2}(u^2 + v^2 + w^2), \tag{6}$$

p is the pressure defined as $p = \rho RT$, where R is the perfect gas constant and T the temperature. Eq. (6) and the perfect gas law can be combined to yield:

$$p = (\gamma - 1)\left[\rho e - \frac{1}{2}\rho(u^2 + v^2 + w^2)\right]. \tag{7}$$

On the other hand, the incompressible Euler equations are:

$$\mathrm{div}(\vec{\boldsymbol{u}}) = 0, \tag{8}$$

$$\rho_0\left[\frac{\partial}{\partial t}\vec{\boldsymbol{u}} + \mathrm{div}(\vec{\boldsymbol{u}} \otimes \vec{\boldsymbol{u}})\right] + \nabla\pi = 0, \tag{9}$$

where ρ_0 is a constant reference density and π the dynamic pressure. The incompressible fluid equations are known to be the singular limit of the compressible Euler equations when the Mach number tends to 0. As an introduction to the computations that will be carried out in Section 3, we recall here how to formally derive this singular limit. The first step of this derivation is performed through the non-dimensionalization of the compressible Euler equations. Let $\rho_i(\boldsymbol{x})$, $\vec{\boldsymbol{u}}_i(\boldsymbol{x})$ and $p_i(\boldsymbol{x})$ be the initial values of the density, velocity and pressure fields. Let $\rho^* = \max_x[\rho_i(\boldsymbol{x})]$, $u^* = \max_x[|\vec{\boldsymbol{u}}_i(\boldsymbol{x})|]$, and let the sound speed scale a^* be defined by: $\rho^*(a^*)^2 = \gamma\max_x[p_i(\boldsymbol{x})]$. Introducing the new non-dimensionalized variables:

$$\tilde{\rho} = \frac{\rho}{\rho^*}, \quad \tilde{\boldsymbol{u}} = \frac{\vec{\boldsymbol{u}}}{u^*}, \quad \tilde{p} = \frac{p}{\rho^*(a^*)^2},$$
$$\tilde{e} = \frac{e}{(a^*)^2}, \quad \tilde{\boldsymbol{x}} = \frac{\boldsymbol{x}}{\delta^*}, \quad \tilde{t} = \frac{tu^*}{\delta^*}, \tag{10}$$

where δ^* is an arbitrary length scale, we obtain the system of non-dimensionalized equations:

$$\frac{\partial}{\partial \tilde{t}}\tilde{\rho} + \operatorname{div}(\tilde{\rho}\tilde{\boldsymbol{u}}) = 0, \tag{11}$$

$$\frac{\partial}{\partial \tilde{t}}\tilde{\rho}\tilde{\boldsymbol{u}} + \operatorname{div}(\tilde{\rho}\tilde{\boldsymbol{u}} \otimes \tilde{\boldsymbol{u}}) + \frac{1}{M_*^2}\nabla\tilde{p} = 0, \tag{12}$$

$$\frac{\partial}{\partial \tilde{t}}\tilde{\rho}\tilde{e} + \operatorname{div}(\tilde{\rho}\tilde{e}\tilde{\boldsymbol{u}} + \tilde{p}\tilde{\boldsymbol{u}}) = 0, \tag{13}$$

where $M_* = u^*/a^*$ is the reference Mach number. The non-dimensionalized state law in Eq. (7) takes the form:

$$\tilde{p} = (\gamma - 1)\left[\tilde{\rho}\tilde{e} - \frac{M_*^2}{2}\tilde{\rho}(\tilde{\boldsymbol{u}}^2 + \tilde{v}^2 + \tilde{w}^2)\right]. \tag{14}$$

We now look for solutions of the system in Eqs. (11)–(13) in the form of asymptotic expansion in power of the Mach number:

$$\tilde{\rho} = \tilde{\rho}_0 + M_*\tilde{\rho}_1 + M_*^2\tilde{\rho}_2 + \ldots$$
$$\tilde{\boldsymbol{u}} = \tilde{\boldsymbol{u}}_0 + M_*\tilde{\boldsymbol{u}}_1 + M_*^2\tilde{\boldsymbol{u}}_2 + \ldots$$
$$\tilde{p} = \tilde{p}_0 + M_*\tilde{p}_1 + M_*^2\tilde{p}_2 + \ldots$$
$$\tilde{e} = \tilde{e}_0 + M_*\tilde{e}_1 + M_*^2\tilde{e}_2 + \ldots$$

Introducing these expressions in Eqs. (11)–(13) and collecting the terms with equal power of M_* we obtain (we have dropped the ˜ for convenience):

(1) Order $1/M_*^2$

$$\nabla p_0 = 0; \tag{15}$$

(2) Order $1/M_*$

$$\nabla p_1 = 0; \tag{16}$$

(3) Order 1

$$\frac{\partial}{\partial t}\rho_0 + \operatorname{div}(\rho_0\boldsymbol{u}_0) = 0, \tag{17}$$

$$\frac{\partial}{\partial t}\rho_0\boldsymbol{u}_0 + \operatorname{div}(\rho_0\boldsymbol{u}_0 \otimes \boldsymbol{u}_0) + \nabla p_2 = 0, \tag{18}$$

$$\frac{\partial}{\partial t}\rho_0 e_0 + \mathrm{div}(\rho_0 e_0 \boldsymbol{u}_0 + p_0 \boldsymbol{u}_0) = 0, \tag{19}$$

while the order 1 state law becomes:

$$p_0 = (\gamma - 1)(\rho_0 e_0).$$

The order $1/M_*^2$ and $1/M_*$ equations imply that the pressure is constant in space up to fluctuations of order M_*^2. Thus, we may write:

$$p(\boldsymbol{x}, t) = P_0(t) + M_*^2 p_2(\boldsymbol{x}, t).$$

In the presence of open boundaries, the thermodynamic pressure P_0 will be imposed and be equal to the exterior pressure. For the sake of simplicity, we assume that the exterior pressure does not change with time, and thus, the thermodynamic pressure P_0 will be a constant in space and time:

$$\frac{\mathrm{d}P_{\mathrm{ext}}}{\mathrm{d}t} = \frac{\mathrm{d}P_0}{\mathrm{d}t} = 0.$$

We deduce from the non-dimensionalized order 1 state law that

$$\frac{\partial \rho_0 e_0}{\partial t} = \nabla \rho_0 e_0 = 0$$

and the energy Eq. (19) degenerates into:

$$\mathrm{div}(\boldsymbol{u}_0) = 0.$$

Introducing this relation into the continuity equation, we see that this implies that the material derivative of the density is zero. Assuming for simplicity that all particle paths come from regions with the same density, we conclude that:

$$\rho_0 = Cte,$$

and that the order 1 system reduces to the following set of equations:

$$\rho_0 = Cte, \tag{20}$$

$$\rho_0 \left[\frac{\partial}{\partial t}\boldsymbol{u}_0 + \mathrm{div}(\boldsymbol{u}_0 \otimes \boldsymbol{u}_0) \right] + \nabla p_2 = 0, \tag{21}$$

$$\mathrm{div}(\boldsymbol{u}_0) = 0. \tag{22}$$

3. The discrete case

Our aim is now to perform a similar analysis of the low Mach number behaviour of the discrete compressible Euler equations, when a flux difference splitting method is used to approximate the system in Eqs. (3)–(5). For simplicity, we consider that we use a regular cartesian grid of uniform mesh size δ in two dimensions: $\boldsymbol{i} = (i, j)$ is the index of the node whose coordinates are $(i\delta, j\delta)$, and we use the notation $v(\boldsymbol{i}) = \{(i-1, j), (i+1, j), (i, j-1), (i, j+1)\}$ or $v(\boldsymbol{i}) = \{N, S, E, W\}$ for labelling the neighbours of the grid node $\boldsymbol{i}$. The cell associated with node $\boldsymbol{i}$ is $C_{\boldsymbol{i}} = [(i-1/2)\delta, (i+1/2)\delta] \times [(j-1/2)\delta, (j+1/2)\delta]$, $\vec{\mathbf{n}}$ is the outward unit normal vector on ∂C_i and we note

$$\vec{\mathbf{n}}_{\boldsymbol{il}} = \frac{\int_{C_i \cap C_l^{\vec{\mathbf{n}}}}}{\delta}.$$

The application of Roe's approximate Riemann solver in a first-order finite volume scheme yields the following set of semi-discrete equations (see Appendix I for details):

$$\delta \frac{\partial}{\partial t}\rho_{\boldsymbol{i}} + \frac{1}{2}\sum_{\boldsymbol{l}\in v(\boldsymbol{i})} \rho_{\boldsymbol{l}} \vec{\mathbf{u}}_{\boldsymbol{l}} \cdot \vec{\mathbf{n}}_{\boldsymbol{il}} + \frac{1}{2}\sum_{\boldsymbol{l}\in v(\boldsymbol{i})} |\, U_{\boldsymbol{il}} \,| \left(\Delta_{\boldsymbol{il}}\rho - \frac{\Delta_{\boldsymbol{il}} p}{a_{\boldsymbol{il}}^2} \right) + \rho_{\boldsymbol{il}} \frac{U_{\boldsymbol{il}}}{a_{\boldsymbol{il}}} \Delta_{\boldsymbol{il}} U + \frac{\Delta_{\boldsymbol{il}} p}{a_{\boldsymbol{il}}} = 0, \tag{23}$$

$$\delta \frac{\partial}{\partial t}\rho_{\boldsymbol{i}} u_{\boldsymbol{i}} + \frac{1}{2}\sum_{\boldsymbol{l}\in v(\boldsymbol{i})} \rho_{\boldsymbol{l}} u_{\boldsymbol{l}} \vec{u}_{\boldsymbol{l}} \cdot \vec{n}_{\boldsymbol{il}} + p_{\boldsymbol{l}} (n_x)_{\boldsymbol{il}} + \frac{1}{2}\sum_{\boldsymbol{l}\in v(\boldsymbol{i})} |\, U_{\boldsymbol{il}} \,| \left(\Delta_{\boldsymbol{il}}\rho - \frac{\Delta_{\boldsymbol{il}} p}{a_{\boldsymbol{il}}^2} \right) u_{\boldsymbol{il}} + \rho_{\boldsymbol{il}} \frac{U_{\boldsymbol{il}}}{a_{\boldsymbol{il}}} u_{\boldsymbol{il}} \Delta_{\boldsymbol{il}} U - \rho_{\boldsymbol{il}} |\, U_{\boldsymbol{il}} \,| (n_y)_{\boldsymbol{il}} \Delta_{\boldsymbol{il}} V + \frac{(U n_x + u)_{\boldsymbol{il}}}{a_{\boldsymbol{il}}} \Delta_{\boldsymbol{il}} p + \rho_{\boldsymbol{il}} a_{\boldsymbol{il}} (n_x)_{\boldsymbol{il}} \Delta_{\boldsymbol{il}} U = 0, \tag{24}$$

$$\delta \frac{\partial}{\partial t}\rho_{\boldsymbol{i}} v_{\boldsymbol{i}} + \frac{1}{2}\sum_{\boldsymbol{l}\in v(\boldsymbol{i})} \rho_{\boldsymbol{l}} v_{\boldsymbol{l}} \vec{u}_{\boldsymbol{l}} \cdot \vec{n}_{\boldsymbol{il}} + p_{\boldsymbol{l}} (n_y)_{\boldsymbol{il}} + \frac{1}{2}\sum_{\boldsymbol{l}\in v(\boldsymbol{i})} |\, U_{\boldsymbol{il}} \,| \left(\Delta_{\boldsymbol{il}}\rho - \frac{\Delta_{\boldsymbol{il}} p}{a_{\boldsymbol{il}}^2} \right) v_{\boldsymbol{il}} + \rho_{\boldsymbol{il}} \frac{U_{\boldsymbol{il}}}{a_{\boldsymbol{il}}} v_{\boldsymbol{il}} \Delta_{\boldsymbol{il}} U + \rho_{\boldsymbol{il}} |\, U_{\boldsymbol{il}} \,| (n_x)_{\boldsymbol{il}} \Delta_{\boldsymbol{il}} V + \frac{(U n_y + v)_{\boldsymbol{il}}}{a_{\boldsymbol{il}}} \Delta_{\boldsymbol{il}} p + \rho_{\boldsymbol{il}} a_{\boldsymbol{il}} (n_y)_{\boldsymbol{il}} \Delta_{\boldsymbol{il}} U = 0, \tag{25}$$

$$\delta\frac{\partial}{\partial t}\rho_i e_i+\frac{1}{2}\sum_{l\in v(i)}(\rho_l e_l+p_l)\vec{u}_l\cdot\vec{n}_{il}$$

$$+\frac{1}{2}\sum_{l\in v(i)}\mid U_{il}\mid\left(\Delta_{il}\rho-\frac{\Delta_{il}p}{a_{il}^2}\right)\left(\frac{u_{il}^2+v_{il}^2}{2}\right)+\rho_{il}\frac{U_{il}}{a_{il}}h_{il}\Delta_{il}U$$

$$+\rho_{il}\mid U_{il}\mid V_{il}\Delta_{il}V+\frac{(h+U^2)_{il}}{a_{il}}\Delta_{il}p+\rho_{il}a_{il}U_{il}\Delta_{il}U=0, \tag{26}$$

where we have introduced the additional notations:

$$\Delta_{il}(\cdot)=(\cdot)_i-(\cdot)_l;\quad U=\vec{\boldsymbol{u}}\cdot\vec{\mathbf{n}};\quad V=-un_y+vn_x;\ \text{and}\ \rho_{il}=\sqrt{\rho_i\rho_l}.$$

$(h,\ u,\ v)_{il}$ denotes the Roe average between the states $(h,\ u,\ v)_i$ and $(h,\ u,\ v)_l$ defined by:

$$h_{il}=\frac{h_i\sqrt{\rho_i}+h_l\sqrt{\rho_l}}{\sqrt{\rho_i}+\sqrt{\rho_l}};\quad (u,\ v)_{il}=\frac{(u,\ v)_i\sqrt{\rho_i}+(u,\ v)_l\sqrt{\rho_l}}{\sqrt{\rho_i}+\sqrt{\rho_l}},$$

with h the specific enthalpy given by:

$$h=e+\frac{p}{\rho}.$$

The average sound speed a_{il} is given by:

$$a_{il}^2=(\gamma-1)\left[h_{il}-\frac{1}{2}(u_{il}^2+v_{il}^2)\right].$$

Note that the present analysis is not restricted to the use of the Roe scheme, but can be extended to all the schemes that can be cast under the form of Eq. (1), with a matrix **A** that is the Jacobian of the continuous fluxes evaluated at some average between $\boldsymbol{i}$ and $\boldsymbol{l}$. In the present low Mach number context, the use of the Roe scheme is only justified by the fact that the algebraic properties of the Roe averages simplify the discrete equations.

Now, using the same dimensionless variables as in Section 2 [see Eq. (10)] we obtain from the system in Eqs. (23)–(26):

$$\frac{1}{2M_*}\sum_{l\in v(i)}\frac{\Delta_{il}p}{a_{il}}+$$

$$\tilde{\delta}\frac{\mathrm{d}}{\mathrm{d}t}\rho_i+\frac{1}{2}\sum_{l\in v(i)}\rho_l\vec{u}_l\cdot\vec{n}_{il}+\mid U_{il}\mid\left(\Delta_{il}\rho-\frac{\Delta_{il}p}{a_{il}^2}\right)+$$

$$\frac{M_*}{2}\sum_{l\in v(i)}\rho_{il}\frac{U_{il}}{a_{il}}\Delta_{il}U=0, \tag{27}$$

$$\frac{1}{2M_*^2}\sum_{l\in v(i)} p_l(n_x)_{il}+$$
$$\frac{1}{2M_*}\sum_{l\in v(i)}\frac{Un_x+u)_{il}}{a_{il}}\Delta_{il}p+\rho_{il}a_{il}(n_x)_{il}\Delta_{il}U+$$
$$\tilde{\delta}\frac{\mathrm{d}}{\mathrm{d}t}\rho_i u_i+\frac{1}{2}\sum_{l\in v(i)}\rho_l u_l\vec{u}_l\cdot\vec{\mathbf{n}}_{il}+\mid U_{il}\mid\left(\Delta_{il}\rho-\frac{\Delta_{il}p}{a_{il}^2}\right)u_{il}-\rho_{il}\mid U_{il}\mid(n_y)_{il}\Delta_{il}V+$$
$$\frac{M_*}{2}\sum_{l\in v(i)}\rho_{il}\frac{U_{il}}{a_{il}}u_{il}\Delta_{il}U=0, \tag{28}$$

$$\frac{1}{2M_*^2}\sum_{l\in v(i)} p_l(n_y)_{il}+$$
$$\frac{1}{2M_*}\sum_{l\in v(i)}\frac{(Un_y+v)_{il}}{a_{il}}\Delta_{il}p+\rho_{il}a_{il}(n_y)_{il}\Delta_{il}U+$$
$$\tilde{\delta}\frac{\mathrm{d}}{\mathrm{d}t}\rho_i v_i+\frac{1}{2}\sum_{l\in v(i)}\rho_l v_l\vec{u}_l\cdot\vec{\mathbf{n}}_{il}+\mid U_{il}\mid\left(\Delta_{il}\rho-\frac{\Delta_{il}p}{a_{il}^2}\right)v_{il}+\rho_{il}\mid U_{il}\mid(n_x)_{il}\Delta_{il}V+$$
$$\frac{M_*}{2}\sum_{l\in v(i)}\rho_{il}\frac{U_{il}}{a_{il}}v_{il}\Delta_{il}U=0, \tag{29}$$

$$\frac{1}{2M_*}\sum_{l\in v(i)}\frac{h_{il}}{a_{il}}\Delta_{il}p+$$
$$\tilde{\delta}\frac{\mathrm{d}}{\mathrm{d}t}\rho_i e_i+\frac{1}{2}\sum_{l\in v(i)}(\rho_l e_l+p_l)\vec{u}_l\cdot\vec{n}_{il}+$$
$$\frac{M_*}{2}\sum_{l\in v(i)}\frac{U_{il}^2}{a_{il}}\Delta_{il}p+\rho_{il}a_{il}U_{il}\Delta_{il}U+\rho_{il}\frac{U_{il}}{a_{il}}h_{il}\Delta_{il}U+$$
$$\frac{M_*^2}{2}\sum_{l\in v(i)}\mid U_{il}\mid\left(\Delta_{il}\rho-\frac{\Delta_{il}p}{a_{il}^2}\right)\left(\frac{u_{il}^2+v_{il}^2}{2}\right)+\rho_{il}\mid U_{il}\mid V_{il}\Delta_{il}V=0, \tag{30}$$

while the dimensionless equation of state is given by Eq. (14).

Following the method used in the continuous case, we next expand all the variables in power of the reference Mach number M_*:

$$(\cdot)=(\cdot)_0+M_*(\cdot)_1+M_*^2(\cdot)_2+\ldots \tag{31}$$

and introduce these expansions into the system in Eqs. (27)–(30). Collecting terms with equal power of M_*, we obtain:

(1) Order $1/M_*^2$

$$p_N^0 - p_S^0 = 0; \quad p_E^0 - p_W^0 = 0; \tag{32}$$

(2) Order $1/M_*$

(a) continuity equation

$$\frac{1}{2}\sum_{l\in v(i)} \frac{\Delta_{il} p^0}{a_{il}^0} = 0, \tag{33}$$

(b) horizontal momentum equation

$$\frac{1}{2}\sum_{l\in v(i)} \frac{(U^0 n_x + u^0)_{il}}{a_{il}^0}\Delta_{il} p^0 + \rho_{il}^0 a_{il}^0 (n_x)_{il}\Delta_{il} U^0 + \sum_{l\in v(i)} p_l^1 (n_x)_{il} = 0, \tag{34}$$

(c) vertical momentum equation

$$\frac{1}{2}\sum_{l\in v(i)} \frac{(U^0 n_y + v^0)_{il}}{a_{il}^0}\Delta_{il} p^0 + \rho_{il}^0 a_{il}^0 (n_y)_{il}\Delta_{il} U^0 + \sum_{l\in v(i)} p_l^1 (n_y)_{il} = 0, \tag{35}$$

(d) energy equation

$$\frac{1}{2}\sum_{l\in v(i)} \frac{h_{il}^0}{a_{il}^0}\Delta_{il} p^0 = 0. \tag{36}$$

Now, let us solve Eqs. (32)–(36), we have:

Lemma 3.1: *Eqs. (32) and (33), or (32) and (36) imply that* $p_l^0 = cte\ \forall l$.

Proof: Eq. (32) implies that p^0 has a four field solution of the form depicted in Fig. 1.

To prove that the spurious pressure mode $p_{i,l}^0 = A$, $p_{i+1,l}^0 = B$, $p_{i,l+1}^0 = C$, $p_{i+1,l+1}^0 = D$ is not actually present in the solution, assume for instance that A is the maximum of the four value A, B, C, D. We note now that the coefficients of Eq. (33) are positive. Thus, all the terms

B	**A**	**B**	**A**	**B**	**A**	
D	**C**	**D**	**C**	**D**	**C**	
B	**A**	**B**	**A**	**B**	**A**	
D	**C**	**D**	**C**	**D**	**C**	

Fig. 1. Four field solution of the $1/M_*^2$ order Eq. (32).

in the sum of Eq. (33) are positive and Eq. (33) cannot equal 0 unless $A = B = C = D$. In other words, the discrete maximum principle applies and necessarily the four values in the set A, B, C, D are equal.

Therefore, we see that the $1/M_*$-order momentum Eqs. (34) and (35) reduce to:

$$p_E^1 - p_W^1 = \rho_{iE}^0 a_{iE}^0 \Delta_{iE} U^0 + \rho_{iW}^0 a_{iW}^0 \Delta_{iW} U^0 \tag{37}$$

and

$$p_N^1 - p_S^1 = \rho_i^0 N a_{iN}^0 \Delta_{iN} U^0 + \rho_{iS}^0 a_{iS}^0 \Delta_{iS} U^0. \tag{38}$$

These equations *do* imply that the order M_* pressure p^1 is *not* a constant. Thus, we have:

Proposition 3.1: *The solutions of the discrete Euler Eqs. (23)–(26) support pressure fluctuations of order* M_*:

$$p(\boldsymbol{x}, t) = P_0(t) + M_* p_1(\boldsymbol{x}, t). \tag{39}$$

This is in clear contrast with the continuous case where pressure fluctuations scale as M_*^2.

Therefore, on a *fixed mesh* (δ = constant), we cannot recover the correct scaling of the pressure with the Mach number. The discrete solutions of Eqs. (23)–(26) exhibit pressure fluctuations that are much larger than in the continuous case. Moreover, the ratio between the numerical pressure fluctuations and the exact ones will increase as the Mach number goes to zero.

In order to illustrate the above theory, we consider a sequence of computations of the flow around a NACA0012 airflow at decreasing Mach number on the same fixed mesh. Fig. 2 shows the pressure fields obtained for three different inflow Mach numbers. In these computations, the inflow velocity is kept constant, equal to unity, while the inflow pressure is increased. To allow a comparison between the pressure fields at different Mach number, Fig. 2 shows the normalized pressure p_{norm} defined as $p_{\text{norm}} = p - p_{\min}/p_{\max} - p_{\min}$. As the Mach number decreases, the results become worse and the solutions do not converge to a reasonable approximation of the incompressible solution. Actually, the $Mach = 0.1$ solution is closer to the incompressible one than is the $Mach = 0.001$ solution. This point had already been noticed [6] by several other investigators.

Fig. 3 that displays the pressure fluctuation $(P_{\max} - P_{\min})/P_{\max}$ vs the inflow Mach number, explains why this behaviour occurs. In perfect agreement with the theoretical predictions, it is easily checked that the pressure fluctuations are proportional to the Mach number. Thus, the accuracy of the numerical results in the incompressible limit is very low, and this accuracy deteriorates as the Mach number decreases.

One possible way to recover a greater accuracy could be to use an improved spatial approximation. In Fig. 3 the results obtained with a second order MUSCL type scheme are also plotted. Although the previous theory does not strictly apply to this case, where the dissipative terms are of fourth order, while the theory has been performed for second-order dissipative terms, it can be seen that the pressure fluctuations still scale approximately with the Mach number and not with its square. Therefore, the use of second-order schemes gives only a marginal improvement with respect to those of the first order.

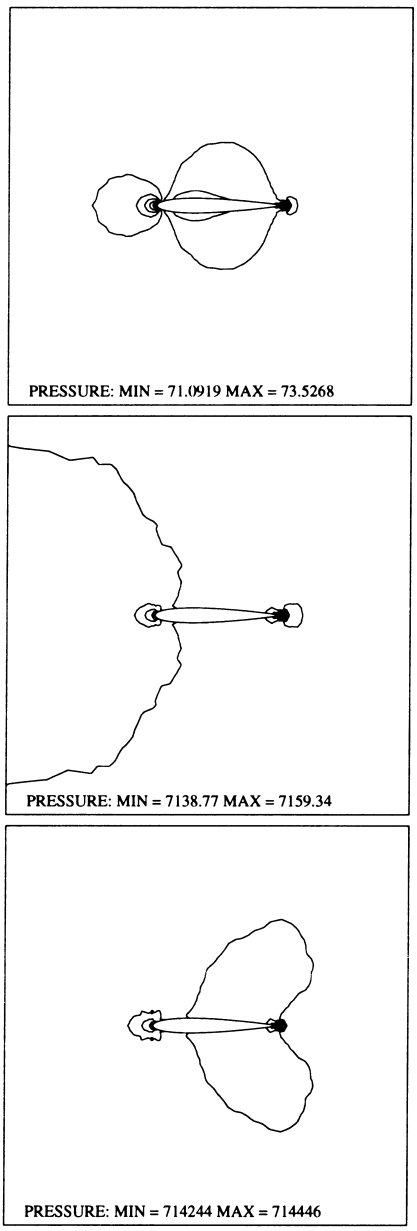

Fig. 2. Isovalues of the pressure, on a 3114 node mesh for $M_\infty = 0.1$ (top), $M_\infty = 0.01$ (middle), $M_\infty = 0.001$ (bottom).

4. Preconditioned dissipation

In this section, we discuss a similar study in the case where Roe's dissipation is modified by preconditioning. Specifically, let $\mathbf{A}(q_{il})$ be the Roe matrix associated to nodes i and $l > / \mathrm{b} >$, we

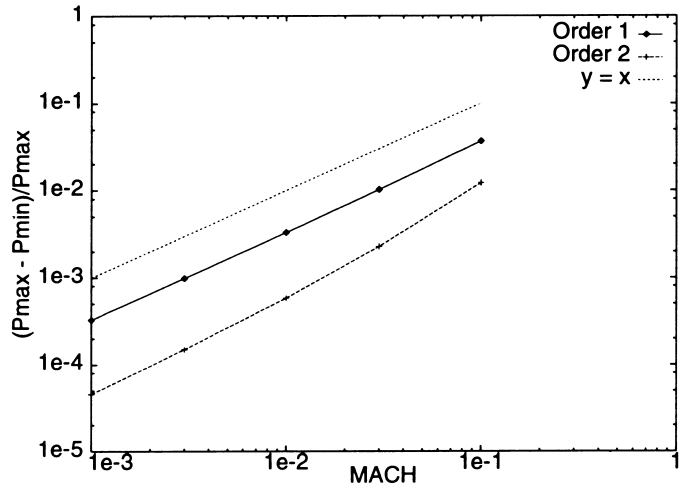

Fig. 3. Pressure fluctuations vs inflow Mach number; solid line: order 1, dashed line: order 2. For comparison, the curve $y = x$ is represented by a dotted line.

change the numerical flux into:

$$\Phi(q_i, q_I, \vec{\mathbf{n}}_{il}) = \frac{\vec{F}(q_i) + \vec{F}(q_i)}{2} \cdot \vec{\mathbf{n}}_{il} + \frac{1}{2}\mathbf{P}(q_{il})^{-1} \mid \mathbf{P}(q_{il})\mathbf{A}(q_{il}) \mid \Delta_{il}q, \tag{40}$$

where $\mathbf{P}$ is the preconditioning matrix. With respect to the original Roe scheme, only the dissipative terms are altered and therefore, the numerical scheme remains a consistant approximation of the time-dependent compressible Euler equations. In this work, we use the preconditioner proposed by Turkel in Ref. [9]. In term of the 'primitive' variables $U = [p, u, v, \ln(p/(\rho^{\gamma}))]$, this preconditioner writes:

$$\mathbf{P} = \begin{pmatrix} \beta^2 & 0 & 0 & 0 \\ 0 & 1 & 0 & 0 \\ 0 & 0 & 1 & 0 \\ 0 & 0 & 0 & 1 \end{pmatrix},$$

where β is a small factor of the order of the Mach number. For the conservative variables $q = [\rho, \rho u, \rho v, \rho e]$ the corresponding form is:

$$\mathbf{P}(q) = \frac{\partial q}{\partial U}\mathbf{P}(U)\frac{\partial U}{\partial q}.$$

To obtain an explicit expression for the stabilization term:

$$\mathbf{P}(q_{il})^{-1} \mid \mathbf{P}(q_{il})\mathbf{A}(q_{il}) \mid \Delta_{il}q$$

close to the expression obtained for the original scheme, we first diagonalize the matrix $\mathbf{P}(q_{il})\mathbf{A}(q_{il})$. Its eigenvalues λ_k (q_{il}) are given by:

$$\begin{aligned}
\lambda_1 &= U_{il},\\
\lambda_2 &= U_{il},\\
\lambda_3 &= \frac{1}{2}[(1+\beta^2)U_{il} + \sqrt{X}],\\
\lambda_4 &= \frac{1}{2}[(1+\beta^2)U_{il} - \sqrt{X}],
\end{aligned} \tag{41}$$

with $X = [(1-\beta^2)\ U_{il}]^2 + 4\beta^2 a_{il}^2$. The product of the eigenvectors of $\mathbf{P}(q_{il})$ $\mathbf{A}(q_{il})$ by $\mathbf{P}(q_{il})^{-1}$ results in expressions that are close to the expressions of the eigenvectors of the Roe's matrix [see equation (A4) of Appendix I]:

$$\mathbf{R}_1(q_{il}) = \begin{bmatrix} 1 \\ u_{il} \\ v_{il} \\ \dfrac{u_{il}^2 + v_{il}^2}{2} \end{bmatrix}, \quad \mathbf{R}_2(q_{il}) = \begin{bmatrix} 0 \\ -(n_y)_{il} \\ (n_x)_{il} \\ V_{il} \end{bmatrix},$$

$$\mathbf{R}_3(q_{il}) = \begin{bmatrix} 1 \\ u_{il} + r(n_x)_{il} \\ v_{il} + r(n_y)_{il} \\ h_{il} + rU_{il} \end{bmatrix}, \quad \mathbf{R}_4(q_{il}) = \begin{bmatrix} 1 \\ u_{il} + s(n_x)_{il} \\ v_{il} + s(n_y)_{il} \\ h_{il} + sU_{il} \end{bmatrix}, \tag{42}$$

where $r = \lambda_3 - U_{il}\beta^2$ and $s = \lambda_4 - U_{il}\beta^2$.

If we now, introduce the coordinate α_k $(\Delta_{il}q)$ of the jump $\Delta_{il}q$ in the basis of the eigenvectors of $\mathbf{P}(q_{il})$ $\mathbf{A}(q_{il})$ whose expressions are:

$$\begin{aligned}
\alpha_1(\Delta_{il}q) &= \Delta_{il}\rho - \frac{\Delta_{il}p}{a_{il}^2},\\
\alpha_2(\Delta_{il}q) &= \rho_{il}\Delta_{il}V,\\
\alpha_3(\Delta_{il}q) &= \frac{1}{\sqrt{X}}\left(\frac{\Delta_{il}p}{r} + \rho_{il}\Delta_{il}U\right),\\
\alpha_4(\Delta_{il}q) &= \frac{1}{\sqrt{X}}\left(\frac{\Delta_{il}p}{-s} - \rho_{il}\Delta_{il}U\right).
\end{aligned} \tag{43}$$

we get:

$$\mathbf{P}(q_{il})^{-1} \mid \mathbf{P}(q_{il})\mathbf{A}(q_{il}) \mid \Delta_{il}q = \sum_{k=1}^{4} \alpha_k(\Delta_{il}) \mid \lambda_k(q_{il}) \mid \mathbf{R}_k(q_{il}),$$

or in developed form:

$$\mathbf{P}(q_{il})^{-1} \mid \mathbf{P}(q_{il})\mathbf{A}(q_{il}) \mid \Delta_{il}q =$$

$$\begin{bmatrix} \mid U_{il} \mid \alpha_1(\Delta_{il}q) & & +d_2\dfrac{\Delta_{il}p}{a_{il}^2} + d_1\rho_{il}\Delta_{il}U \\ \mid U_{il} \mid \alpha_1(\Delta_{il}q)u_{il} & -\rho_{il} \mid U_{il} \mid (n_y)_{il}\Delta_{il}V & +d_4\dfrac{\Delta_{il}p}{a_{il}^2} + d_3\rho_{il}\Delta_{il}U \\ \mid U_{il} \mid \alpha_1(\Delta_{il}q)v_{il} & +\rho_{il} \mid U_{il} \mid (n_x)_{il}\Delta_{il}V & +d_6\dfrac{\Delta_{il}p}{a_{il}^2} + d_5\rho_{il}\Delta_{il}U \\ \mid U_{il} \mid \alpha_1(\Delta_{il}q)\frac{u_{il}^2+v_{il}^2}{2} & +\rho_{il} \mid U_{il} \mid \nabla_{il}\Delta_{il}V & +d_8\dfrac{\Delta_{il}p}{a_{il}^2} + d_7\rho_{il}\Delta_{il}U \end{bmatrix} \tag{44}$$

where

$$d_1 = \frac{U_{il}}{\sqrt{X}}(1+\beta^2), \quad d_2 = \frac{U_{il}^2}{\sqrt{X}}\left(\beta^2 - 1 + \frac{2a_{il}^2}{U_{il}^2}\right), \tag{45}$$

and

$$\begin{aligned} d_3 &= u_{il}d_1 + (n_x)_{il}d_9, & d_4 &= u_{il}d_2 - sr(n_x)_{il}d_1/\beta^2, \\ d_5 &= v_{il}d_1 + (n_y)_{il}d_9, & d_6 &= v_{il}d_2 - sr(n_y)_{il}d_1/\beta^2, \\ d_7 &= h_{il}d_1 + U_{il}d_9, & d_8 &= h_{il}d_2 - srU_{il}d_1/\beta^2, \\ d_9 &= \tfrac{U_{il}^2}{\sqrt{X}}\left(1 - \beta^2 + \frac{2\beta^2 a_{il}^2}{U_{il}^2}\right), \end{aligned} \tag{46}$$

and we have used $|\lambda_3| = \lambda_3$ and $|\lambda_4| = -\lambda_4$ because for low Mach number one can easily check that $\lambda_3 > 0$ and $\lambda_4 < 0$.

Now, using the same dimensionless variables as in the previous cases, we write the resulting scheme in a non-dimensionalized form. For this, we need to non-dimensionalize the parameter β that appears in the preconditioner. Since in practice, this parameter is chosen of the order of the Mach number, we take:

$$\beta = M_*\tilde{\beta},$$

and β is a parameter of order unity. In practice, β is often chosen constant in the whole computational domain, here, we consider the more general case where this quantity can be allowed to become a function of the local variables. We also note that the variable $X = [(1-\beta^2)\ U_{il}]^2 + 4\beta^2 a_{il}^2$ can be evaluated as:

$$X = u_*^2[\tilde{U}_{il}^2(1-\tilde{\beta}^2)^2 + 4\tilde{\beta}^2\tilde{a}_{il}^2],$$

and we introduce for convenience the notation $Y = \tilde{U}_{il}^2\ (1-\beta^2)^2 + 4\beta^2\tilde{a}_{il}^2$, where Y is a variable of order unity; once again, in the equations below, we dropped the symbol $\tilde{}$ to simplify the notations. We then obtain:

$$\frac{1}{2M_*^2}\sum_{l\in v(i)}\frac{2\Delta_{il}p}{\sqrt{Y_{il}}}+$$
$$\tilde{\delta}\frac{d}{dt}\rho_i+\frac{1}{2}\sum_{l\in v(i)}\rho_l\vec{u}_l\cdot\vec{n}_{il}+\mid U_{il}\mid\left(\Delta_{il}\rho-\frac{\Delta_{il}p}{a_{il}^2}\right)-\frac{U_{il}^2}{a_{il}^2}\frac{\Delta_{il}p}{\sqrt{Y_{il}}}+\rho_{il}\frac{U_{il}}{\sqrt{Y_{il}}}\Delta_{il}U+$$
$$\frac{M_*^2}{2}\sum_{l\in v(i)}\beta^2\left(\rho_{il}\frac{U_{il}}{\sqrt{Y_{il}}}\Delta_{il}U+\frac{U_{il}^2}{a_{il}^2}\frac{\Delta_{il}p}{\sqrt{Y_{il}}}\right)=0, \tag{47}$$

$$\frac{1}{2M_*^2}\sum_{l\in v(i)}p_l(n_x)_{il}+\frac{(Un_x+2u)_{il}}{\sqrt{Y_{il}}}\Delta_{il}p+$$
$$\tilde{\delta}\frac{\mathrm{d}}{\mathrm{d}t}\rho_iu_i+\frac{1}{2}\sum_{l\in v(i)}\rho_lu_l\vec{u}_l\cdot\vec{n}_{il}+\mid U_{il}\mid\left(\Delta_{il}\rho-\frac{\Delta_{il}p}{a_{il}^2}\right)u_{il}-\rho_{il}\mid U_{il}\mid(n_y)_{il}\Delta_{il}V+$$
$$\frac{(u+Un_x)_{il}U_{il}+2\beta^2a_{il}^2}{\sqrt{Y_{il}}}\rho_{il}\Delta_{il}U+\frac{\beta^2a_{il}^2U_{il}(n_x)_{il}-u_{il}U_{il}^2}{\sqrt{Y_{il}}}\frac{\Delta_{il}p}{a_{il}^2}+$$
$$\frac{M_*^2}{2}\sum_{l\in v(i)}\beta^2\left[\frac{(u-Un_x)_{il}U_{il}}{\sqrt{Y_{il}}}\rho_{il}\Delta_{il}U+\frac{u_{il}U_{il}^2}{\sqrt{Y_{il}}}\frac{\Delta_{il}p}{a_{il}^2}\right]=0, \tag{48}$$

$$\frac{1}{2M_*^2}\sum_{l\in v(i)}p_l(n_y)_{il}+\frac{(Un_y+2v)_{il}}{\sqrt{Y_{il}}}\Delta_{il}p+$$
$$\tilde{\delta}\frac{d}{dt}\rho_iv_i+\frac{1}{2}\sum_{l\in v(i)}\rho_lv_l\vec{u}_l\cdot\vec{n}_{il}+\mid U_{il}\mid\left(\Delta_{il}\rho-\frac{\Delta_{il}p}{a_{il}^2}\right)v_{il}-\rho_{il}\mid U_{il}\mid(n_y)_{il}\Delta_{il}V+$$
$$(v+Un_y)_{il}U_{\frac{il+2\beta^2a_{il}^2}{\sqrt{Y_{il}}}}\rho_{il}\Delta_{il}U+\frac{\beta^2a_{il}^2U_{il}(n_y)_{il}-v_{il}U_{il}^2}{\sqrt{Y_{il}}}\frac{\Delta_{il}p}{a_{il}^2}+$$
$$\frac{M_*^2}{2}\sum_{l\in v(i)}\beta^2\left[\frac{(v-Un_y)_{il}U_{il}}{\sqrt{Y_{il}}}\rho_{il}\Delta_{il}U+\frac{v_{il}U_{il}^2}{\sqrt{Y_{il}}}\frac{\Delta_{il}p}{a_{il}^2}\right]=0, \tag{49}$$

$$\frac{1}{2M_*^2}\sum_{l\in v(i)}\frac{2h_{il}}{\sqrt{Y_{il}}}\Delta_{il}p+$$
$$\tilde{\delta}\frac{d}{dt}\rho_ie_i+\frac{1}{2}\sum_{l\in v(i)}(\rho_le_l+p_l)\vec{u}_l\cdot\vec{n}_{il}+\frac{(h_{il}+a_{il}^2)}{\sqrt{Y_{il}}}U_{il}^2\frac{\Delta_{il}p}{a_{il}^2}+\frac{h_{il}}{\sqrt{Y_{il}}}U_{il}\rho_{il}\Delta_{il}U+$$
$$\frac{M_*^2}{2}\sum_{l\in v(i)}\mid U_{il}\mid\left(\Delta_{il}\rho-\frac{\Delta_{il}p}{a_{il}^2}\right)\left(\frac{u_{il}^2+v_{il}^2}{2}\right)+\rho_{il}\mid U_{il}\mid V_{il}\Delta_{il}V+\beta^2\frac{(h_{il}+a_{ill}^2)U_{il}^2}{\sqrt{Y_{il}}}\frac{\Delta_{il}p}{a_{il}^2}+$$
$$\frac{U_{il}^3+\beta^2(h_{il}+2a_{il}^2)U_{il}}{\sqrt{Y_{il}}}\rho_{il}\Delta_{il}U-\frac{M_*^4}{2}\sum_{l\in v(i)}\beta^2U_{il}^3\rho_{il}\Delta_{il}U=0. \tag{50}$$

Comparing this system with the analogous one in Eqs. (27)–(30) obtained in the case with no preconditioning, we note that now, dissipation terms of order $1/M_*^2$ appear in the continuity and energy equations, and that all the dissipative terms of order $1/M_*$ have disappeared. This will force the pressure fluctuations to be smaller than in the case with no preconditioning. To see that, we expand now the variables in power of the reference Mach number and introduce these expansions in the Eqs. (47)–(50). We obtain at order $1/M_*^2$:

(1) continuity equation

$$\sum_{l\in v(i)} \frac{\Delta_{il} p^0}{\sqrt{Y^0_{il}}} = 0; \tag{51}$$

(2) horizontal momentum equation

$$\sum_{l\in v(i)} p^0_l (n_x)_{il} + \frac{(U^0 n_x + 2u^0)_{il}}{\sqrt{Y^0_{il}}} \Delta_{il} p^0 = 0; \tag{52}$$

(3) vertical momentum equation

$$\sum_{l\in v(i)} p^0_l (n_y)_{il} + \frac{(U^0 n_y + 2v^0)_{il}}{\sqrt{Y^0_{il}}} \Delta_{il} p^0 = 0; \tag{53}$$

(4) energy equation

$$\sum_{l\in v(i)} \frac{2h^0_{il}}{\sqrt{Y^0_{il}}} \Delta_{il} p^0 = 0, \tag{54}$$

with $Y^0 = (U^0_{il})^2 + 4\beta^2 (a^0_{il})^2$. Let us look for the solutions of Eqs. (51)–(54). This is a system of four homogeneous 'elliptic' difference equations for the N values of the order 1 pressure p^0 at the interior points of the computational domain. Obviously, $p^0 \equiv$constant is a common solution of these four equations. However, depending on the boundary conditions, these equations may also have non-constant solutions, and the problem is to establish that the intersection of the kernels of these four equations is reduced to constant vectors. For general arbitrary boundary conditions, we have not been able to prove this result. However, we give below two important cases where this result can be established.

Firstly, we remark that in Eqs. (51) and (54), the coefficients are positive, therefore, the discrete maximum applies and an interior point cannot be an extremum. Therefore, the extrema of the order 1 pressure field p^0 are on the boundary. Thus, if we assume that the pressure on the boundary is constant up to fluctuations of order M_*^2: $P^{\text{boundary}} = p^0 + M_*^2 p_2^{\text{boundary}}$ with p^0 a constant, then p^0 is constant everywhere in the whole domain.

We now proceed to show the same result if the order 1 density ρ_0 is constant on the boundary of the computational domain. Assume that the p^0 pressure is not constant and denote $\boldsymbol{i}$ the point where the maximum value of the pressure is attained (this point always

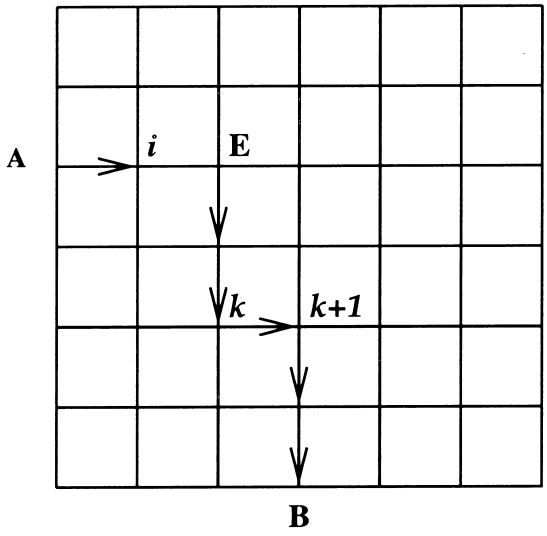

Fig. 4. Path connecting points with decreasing pressures.

exists because there is a finite number of computational nodes). As the maximum principle applies, this point is a neighbour of a boundary node. To fix the idea, assume that this boundary is the left one (see Fig. 4). As the pressure in $\boldsymbol{i}$ is maximum, the differences $\Delta_{il}p^0$ for $\boldsymbol{l} \in \{N, S, E\}$ are positive and this implies that $p^0(A) > p_i^0$ (this is indicated by a '>' symbol on Fig. 4). Now consider Eq. (51), or (54), written at nodes E for instance, because $p_l^0 > p^0(E)$ there must be at least one neighbour of E whose pressure is less than the pressure in E. Repeating the argument for this node, we see that we can construct a path $\mathcal{P} = \{A, \boldsymbol{i}, E, \ldots, \boldsymbol{k}, \boldsymbol{k}+1, \ldots\}$ such that for any $\boldsymbol{k}$ in this list $p_k^0 > p_{k+1}^0$. Since this path cannot make closed loops, it necessarily ends on the boundary. Let us call B the point of the boundary where it ends. Obviously we have $p^0(A) > p^0(B)$.

We remark now that for any interior point, we can rewrite the system of Eqs. (51)–(54) in the form of a system of four equations for the four unknowns $\Delta_{il}p^0$. Since the coefficients of the three Eqs. (51)–(53) are obviously different and arbitrary (they depend on the velocity field), the only possible way for this system to have a non-zero solution is that Eq. (54) is proportional to Eq. (51). This implies that the four values h_{il}^0 are equal. Since h_{il}^0 is an average of the value of h^0 in $\boldsymbol{i}$ and $\boldsymbol{l}$, we make the reasonable assumption that this implies that the four values h_{il}^0 are equal. Now, considering again the path $\mathcal{P}$ we see that this implies that the specific enthalpy h^0 is constant along this path. However, it is easily checked from the order 1 state law that the order 1 specific enthalpy h^0 is defined by $h^0 = \gamma p^0/(\gamma - 1)\rho^0$. This, if $p^0(A) > p^0(B)$, $h^0(A) = h^0(B)$ implies that $\rho^0(A) > \rho^0(B)$, but this is impossible since we have assumed that the density is constant on the boundary.

We also remark from the previous proof, that if the temperature field is not constant in the computational domain, then the h_{il}^0 will be different, and then the argument given above shows that the p^0 pressure field is constant. We collect these results in:

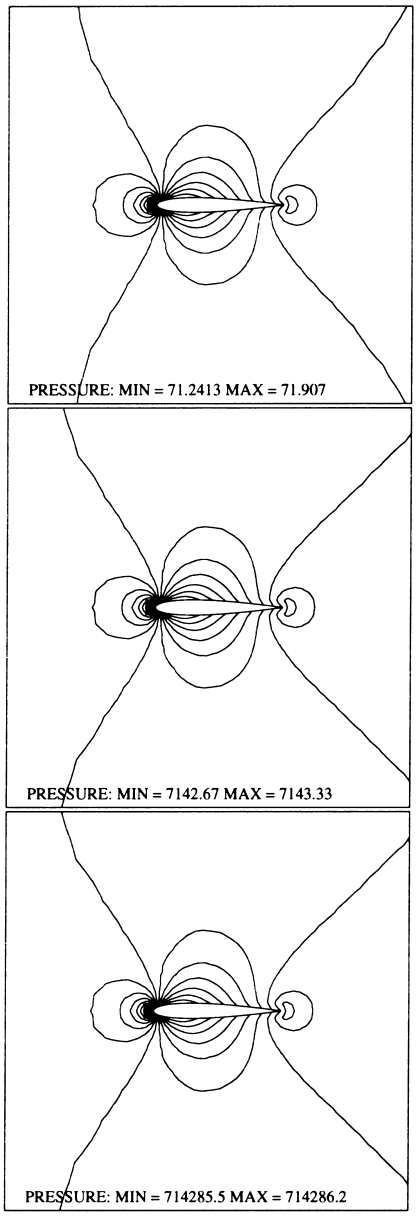

Fig. 5. Isovalues of the pressure, on a 3114 node mesh for $M_\infty = 0.1$ (top), $M_\infty = 0.01$ (middle), $M_\infty = 0.001$ (bottom). Preconditioned dissipation.

Lemma 4.1: *Assume either that:*

(i) *The order 1 temperature field* T^0 *is not constant*;
(ii) *The order 1 pressure* p^0 *is constant on the boundary;* or

(iii) *The order 1 density ρ^0 is constant on the boundary, then the $1/M_*^2$ Eqs. (51)–(54) imply that $p_l^0 = cte\ \forall l$.*

Since there are no $1/M_*$ terms in the Eqs. (47)–(50), the order $1/M_*$ equations that result from the expansion in Eq. (31) are totally identical to the order $1/M_*^2$ equations with p^0 replaced by p^1. Therefore, the same argument as for the order 0 pressure can be used and we have:

Proposition 4.1: *Under the assumptions of lemma 4.1, the solutions of the discrete equations with preconditioned dissipation support pressure fluctuations of order M_*^2:*

$$p(\boldsymbol{x}, t) = P_0(t) + M_*^2 p_2(\boldsymbol{x}, t). \tag{55}$$

Remark: Comparing the case of the preconditioned dissipation with the one of the original Roe scheme, we note that there is an important difference in the *structure* of the order $1/M_*^2$ and $1/M_*$ equations. In the original Roe scheme, the $1/M_*$ equations link the pressure differences with the velocity differences. A consequence is that the order M_* pressure p^1 *cannot* be constant. On the other hand, for the preconditioned dissipation, the order $1/M_*^2$ equations involve only the pressure differences and $p^0 = \text{constant}$ is a trivial solution of each individual equation. Moreover, this system can be cast in the form of a system of four equations for the four unknowns $\Delta_{il}p^0$. A common solution of these four equations is $\Delta_{il}p^0 = 0$. Thus, the only possibility to get a non-constant pressure would be that the determinant of this system is zero, or in other terms not only that the kernels of these four equations contain non-zero vectors, but that the intersection of these kernels is not void. We believe (without proof) that this situation is very unlikely. However, we cannot exclude *a priori* this case: the existence of spurious pressure modes is a well-known problem for the approximation of the equations of incompressible flows, and experience gained in this domain induces one to be careful before ruling out the possibility of the existence of spurious pressure modes in the solution of the system in Eqs. (51)–(54). At least, lemma 4.1 shows that for reasonable assumptions on the behaviour of the pressure or density fields on the boundaries, the system cannot have such a behaviour.

To conclude this section, we return to the numerical experiments performed in Section 3. Fig. 5 presents the pressure fields for the same three decreasing inflow Mach number than in Fig. 2 on the same fixed mesh. In contrast to the results obtained with the original Roe scheme, we note now that the solutions converge to a unique solution (actually, the isovalues for these three Mach numbers are almost undistinguishable). Fig. 6 presents the pressure fluctuations with respect to the Mach number. As in the previous section, the agreement with the theory is remarkable: the pressure fluctuations scale exactly with the square of the Mach number as in the continuous case.

5. Conclusion

Using an asymptotic analysis of the discrete upwind approximation of the compressible Euler equations, we provide a detailed explanation of the mechanism that produces the failure of compressible code to compute very subsonic flows. In the low Mach number limit, the trouble comes from the fact that the discrete equations support pressure fluctuations of the

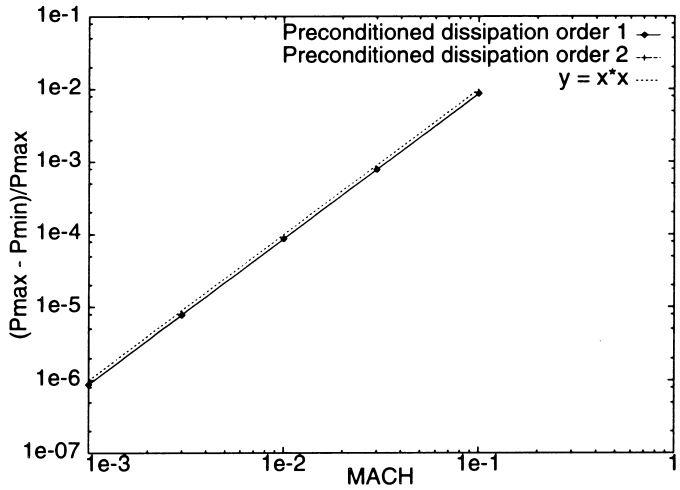

Fig. 6. Pressure fluctuations vs inflow Mach number; solid line: order 1, dashed line: order 2. For comparison, the curve $y = x^2$ is represented by a dotted line.

order of the Mach number, while in the solutions of the continuous equations, the pressure scales with the *square* of the Mach number. The theory is totally confirmed by numerical experiments. We next examine the case where the numerical dissipation is altered with the help of the preconditioning matrix proposed in Ref. [9]. For this latter case, we show that the solution of the discrete equations possesses pressure fluctuations of the correct magnitude. Again, numerical experiments confirm the theoretical results.

Appendix A

A.1. Roe's Approximate Riemann Solver

Let us write the 2D compressible Euler Eqs. (3)–(5) in the conservative form:

$$\frac{\partial q}{\partial t} + \nabla \cdot \vec{\mathbf{F}}(q) = 0,$$
$$\vec{\mathbf{F}}(q) = \begin{bmatrix} F_1(q) \\ F_2(q) \end{bmatrix}, \tag{A1}$$

where

$$q = \begin{bmatrix} \rho \\ \rho u \\ \rho v \\ \rho e \end{bmatrix}, \quad F_1(q) = \begin{bmatrix} \rho u \\ \rho u^2 + p \\ \rho uv \\ (\rho e + p)u \end{bmatrix}, \quad F_2(q) = \begin{bmatrix} \rho v \\ \rho uv \\ \rho v^2 + p \\ (\rho e + p)v \end{bmatrix}. \tag{A2}$$

Integrating these equations on a control volume C_i we get:

$$\delta^2 \frac{\mathrm{d}q_i}{\mathrm{d}t} + \sum_{l \in \nu(i)} \delta\Phi(q_i, q_l, \vec{\mathbf{n}}_{il}) = 0, \tag{A3}$$

where $\Phi(q_i, q_l, \vec{\mathbf{n}}_{il})$, the numerical flux function approximates

$$\frac{1}{\delta} \int_{\partial C_i \cap \partial C_l} \vec{F} \cdot \vec{\mathbf{n}} \, \mathrm{d}l.$$

For Roe scheme, this function is defined by:

$$\Phi(q_i, q_l, \vec{\mathbf{n}}_{il}) = \frac{\vec{F}(q_i) + \vec{F}(q_{il})}{2} \cdot \vec{\mathbf{n}}_{il} + \frac{1}{2} \mid \mathbf{A}(q_{il}, \vec{\mathbf{n}}_{il}) \mid \Delta_{il} q,$$

where the matrix $\mathbf{A}(q_{il}, \vec{\mathbf{n}}_{il})$ satisfies the following property:

$$\mathbf{A}(q_{il}, \vec{\mathbf{n}}_{il}) \Delta_{il} q = [\vec{F}(q_i) - \vec{F}(q_l)] \cdot \vec{\mathbf{n}}_{il}.$$

If we introduce the eigenvectors of matrix $\mathbf{A}(q_{il}, \vec{\mathbf{n}}_{il})$:

$$\mathbf{R}_1(q_{il}) = \begin{bmatrix} 1 \\ u_{il} \\ v_{il} \\ \dfrac{u_{il}^2 + v_{il}^2}{2} \end{bmatrix}, \quad \mathbf{R}_2(q_{il}) = \begin{bmatrix} 0 \\ -(\mathbf{n}_y)_{il} \\ (\mathbf{n}_x)_{il} \\ V_{il} \end{bmatrix},$$

$$\mathbf{R}_3(q_{il}) = \begin{bmatrix} 1 \\ u_{il} + a_{il}(n_x)_{il} \\ v_{il} + a_{il}(n_y)_{il} \\ h_{il} + a_{il} U_{il} \end{bmatrix}, \quad \mathbf{R}_4(q_{il}) = \begin{bmatrix} 1 \\ u_{il} - a_{il}(n_x)_{il} \\ v_{il} - a_{il}(n_y)_{il} \\ h_{il} - a_{il} U_{il} \end{bmatrix}, \tag{A4}$$

where

$$U_{il} = u_{il}(\mathbf{n}_x)_{il} + v_{il}(\mathbf{n}_y)_{il}$$
$$V_{il} = -u_{il}(\mathbf{n}_y)_{il} + v_{il}(\mathbf{n}_x)_{il}.$$

These eigenvectors for a complete base of $\mathbb{R}^4$ and any vector $\mathbf{X} = (X_1, X_2, X_3, X_4)^t$ can be written as:

$$\mathbf{X} = \sum_{k=1}^{4} \alpha_k(\mathbf{X}) \mathbf{R}_k,$$

where the coordinates α_k in this base are defined by:

$$\alpha_1 = X_1 - \frac{\varepsilon}{a_{il}^2}, \quad \alpha_2 = \mathcal{B},$$
$$\alpha_3 = \frac{1}{2}\left(\frac{\varepsilon}{a_{il}^2} + \frac{\mathcal{A}}{a_{il}}\right), \quad \alpha_4 = \frac{1}{2}\left(\frac{\varepsilon}{a_{il}^2} - \frac{\mathcal{A}}{a_{il}}\right), \tag{A5}$$

with

$$\varepsilon = (\gamma - 1)\left(X_4 - v_{il}X_3 - u_{il}X_2 + \frac{u_{il}^2 + v_{il}^2}{2}X_1\right),$$
$$\mathcal{A} = (n_x)_{il}X_2 + (n_y)_{il}X_3 - U_{il}X_1,$$
$$\mathcal{B} = -(n_y)_{il}X_2 + (n_x)_{il}X_3 - V_{il}X_1. \tag{A6}$$

As remarked by Abgrall in Ref. [14], for any $D \neq 0$ the Δ_{il} operator obeys the following rules:

$$\Delta_{il}(ab) = \underline{a}\Delta_{il}b + \overline{b}\Delta_{il}a$$

with

$$\underline{a} = \frac{a_i + Da_l}{1 + D}, \quad \overline{a} = \frac{a_l + Da_i}{1 + D}.$$

Moreover if $D = \sqrt{\rho_i}/\sqrt{\rho_l}$, we have the additional property:

$$\underline{\rho a} = \underline{\rho}\,\overline{a}. \tag{A7}$$

This simplifies to some extent the expression of the numerical dissipation, since we obtain:

$$\alpha_1(\Delta_{il}q) = \Delta_{il}\rho - \frac{\Delta_{il}p}{a_{il}^2},$$
$$\alpha_2(\Delta_{il}q) = \rho_{il}\Delta_{il}V,$$
$$\alpha_3(\Delta_{il}q) = \frac{1}{2a_{il}}\left(\frac{\Delta_{il}p}{a_{il}} + \rho_{il}\Delta_{il}U\right),$$
$$\alpha_4(\Delta_{il}q) = \frac{1}{2a_{il}}\left(\frac{\Delta_{il}p}{a_{il}} - \rho_{il}\Delta_{il}U\right). \tag{A8}$$

Writing the numerical dissipation under the form:

$$|\,\mathbf{A}(q_{il}, \vec{\mathbf{n}}_{il})\,|\,\Delta_{il}q = \sum_{k=1}^{4} \alpha_k(\Delta_{il}q)\,|\,\lambda_k(q_{il})\,|\,\mathbf{R}_k(q_{il}), \tag{A9}$$

with the eigenvalue $\lambda_k\,(q_{il})$ given by:

$$\lambda_1 = U_{il}, \quad \lambda_2 = U_{il},$$
$$\lambda_3 = U_{il} + a_{il}, \quad \lambda_4 = U_{il} - a_{il}, \tag{A10}$$

we then obtain:

$$
|\mathbf{A}(q_{il})|\,\Delta_{il}q =
\begin{bmatrix}
|U_{il}|\,\alpha_1(\Delta_{il}q) & & +d_2\dfrac{\Delta_{il}p}{a_{il}^2} & +d_1\rho_{il}\Delta_{il}U \\
|U_{il}|\,\alpha_1(\Delta_{il}q)u_{il} & -\rho_{il}\,|U_{il}|\,(n_y)_{il}\Delta_{il}V & +d_4\dfrac{\Delta_{il}p}{a_{il}^2} & +d_3\rho_{il}\Delta_{il}U \\
|U_{il}|\,\alpha_1(\Delta_{il}q)v_{il} & +\rho_{il}\,|U_{il}|\,(n_x)_{il}\Delta_{il}V & +d_6\dfrac{\Delta_{il}p}{a_{il}^2} & +d_5\rho_{il}\Delta_{il}U \\
|U_{il}|\,\alpha_1(\Delta_{il}q)\frac{u_{il}^2+v_{il}^2}{2} & +\rho_{il}\,|U_{il}|\,V_{il}\Delta_{il}V & +d_8\dfrac{\Delta_{il}p}{a_{il}^2} & +d_7\rho_{il}\Delta_{il}U
\end{bmatrix},
\tag{A11}
$$

with

$$
\begin{aligned}
&d_1 = \tfrac{U_{il}}{a_{il}}, && d_2 = a_{il},\\
&d_3 = \tfrac{U_{il}}{a_{il}}u_{il} + a_{il}(n_x)_{il}, && d_4 = a_{il}(Un_x + u)_{il},\\
&d_5 = \tfrac{U_{il}}{a_{il}}v_{il} + a_{il}(n_y)_{il}, && d_6 = a_{il}(Un_y + v)_{il},\\
&d_7 = U_{il}\left(\tfrac{h_{il}}{a_{il}} + a_{il}\right), && d_8 = a_{il}(h + U^2)_{il}.
\end{aligned}
\tag{A12}
$$

References

[1] Klein R. Semi-implicit extension of a Godunov-type scheme based on low Mach number asymptotics I: one-dimensional flow. Journal of Computational Physics 1995;121:213–37.

[2] Klainerman S, Majda A. Compressible and incompressible fluids. Communications on Pure and Applied Mathematics 1982;35:629–53.

[3] Kreiss H-O. Problems with different time scales for partial differential equations. Communications on Pure and Applied Mathematics 1980;33:399–440.

[4] Gustafsson B. Asymptotic expansions for hyperbolic problems with different time scales. SIAM Journal of Numerical Analysis 1980;17:623–34.

[5] Browning G, Kreiss H-O. Problems with different time scales for non-linear partial differential equations. SIAM Journal of Applied Mathematics 1982;42:704–18.

[6] Volpe G. Performance of compressible flow codes at low Mach number. AIAA Journal 1993;31:49–56.

[7] Godfrey AG, Walters RW, van Leer B. Preconditioning for the Navier–Stokes equations with finite-rate chemistry, AIAA paper 93-0535. 31st Aerospace Sciences Meeting and Exhibition, Reno, Nevada, 1993.

[8] Turkel E, Fiterman A, van Leer B. Preconditioning and the limit of the compressible to the incompressible flow equations for finite difference schemes. In: Caughey DA, Hafez MM, editors. Frontiers of Computational Fluid Dynamics 1994. Wiley, Chichester, 1994:215–234.

[9] Turkel E. Preconditioned methods for solving the incompressible and low speed compressible equations. Journal of Computational Physics 1987;72:277–98.

[10] Turkel E. Review of preconditioning methods for fluid dynamics. Applied Numerical Mathematics 1993;12:257–84.

[11] Choi Y-H, Merkle CL. The application of preconditioning in viscous flows. Journal of Computational Physics 1993;105:207–23.

[12] Turkel E, Radespiel R, Kroll N. Assessment of preconditioning methods for multidimensional aerodynamics. Computers and Fluids 1997;26:613–34.

[13] Viozat C. Implicit upwind schemes for low Mach number compressible flows, Technical Report 3084. INRIA, 1997.

[14] Abgrall R. An extension of Roe's upwind scheme to algebraic equilibrium real gas models. Computers and Fluids 1991;19:171–82.